

## Eu<sup>2+</sup>、Mn<sup>2+</sup>、Sr<sup>2+</sup>掺杂 BaMgAl<sub>10</sub>O<sub>17</sub> 的燃烧法合成及光致发光性能

张长伟<sup>1</sup> 丁艳花<sup>1</sup> 张 娜<sup>\*,1</sup> 张建勇<sup>\*,2</sup> 房永征<sup>1</sup> 张 骋<sup>1</sup>

(<sup>1</sup> 上海应用技术大学材料科学与工程学院, 上海 201418)

(<sup>2</sup> 上海应用技术大学化学与环境工程工程学院, 上海 201418)

**摘要:** 在 600 °C 温度下, 采用液相燃烧法合成了 Sr<sup>2+</sup>、Eu<sup>2+</sup> 和 Mn<sup>2+</sup> 三掺的 BaMgAl<sub>10</sub>O<sub>17</sub> (BAM) 蓝绿荧光粉。用 XRD、SEM 和荧光光谱仪分别分析和表征该荧光粉的物相、形貌和光致发光性能。结果表明, 液相燃烧法合成 BAM 的温度明显低于传统的高温固相合成法; 合成的纳米棒均匀、无团聚现象; 荧光光谱仪分析表明 Eu<sup>2+</sup>、Mn<sup>2+</sup> 离子间存在能量传递, 且 Sr<sup>2+</sup> 能有效提高 BAM 的发光强度, 约为固相法制备荧光强度的 1.8 倍。BAM:0.1Eu<sup>2+</sup>, 0.04Mn<sup>2+</sup>, 0.05Sr<sup>2+</sup> 色坐标为 (0.146, 0.250), 属于蓝绿光。

**关键词:** 燃烧合成法; BAM; Eu<sup>2+</sup>, Mn<sup>2+</sup>; 发光材料; 蓝绿色荧光粉

中图分类号: O614.33\*8; O614.7\*11; O614.23\*2

文献标识码: A

文章编号: 1001-4861(2016)12-2075-07

DOI: 10.11862/CJIC.2016.237

## Eu<sup>2+</sup>, Mn<sup>2+</sup>, Sr<sup>2+</sup> Tri-doped BaMgAl<sub>10</sub>O<sub>17</sub> Phosphor: Solution Combustion Synthesis and Photoluminescence Properties

ZHANG Chang-Wei<sup>1</sup> DING Yan-Hua<sup>1</sup> ZHANG Na<sup>\*,1</sup>

ZHANG Jian-Yong<sup>\*,2</sup> FANG Yong-Zheng<sup>1</sup> ZHANG Cheng<sup>1</sup>

(<sup>1</sup> School of Materials Science and Engineering, Shanghai Institute of Technology, Shanghai 201418, China)

(<sup>2</sup> School of Chemical and Environmental Engineering, Shanghai Institute of Technology, Shanghai 201418, China)

**Abstract:** Sr<sup>2+</sup>, Eu<sup>2+</sup> and Mn<sup>2+</sup> tri-doped BaMgAl<sub>10</sub>O<sub>17</sub> (BAM) phosphors that emitting the blue-green light are prepared by solution combustion synthesis at 600 °C. X-ray diffraction (XRD), scanning electron microscopy (SEM) and photoluminescence (PL) are employed to measure the powders crystallinity, morphology and luminescent properties, respectively. The results show that the formation temperature of the BAM phase by the solution combustion synthesis (SCS) method is significantly lower than that of a high temperature solid state (HTS) reaction. The nanorods of SBAM: Eu<sup>2+</sup>, Mn<sup>2+</sup> without aggregation and well distribution are synthesized successfully. The well-dispersed morphology of the SCS-derived phosphors is beneficial to the improvement of PL property. While Sr<sup>2+</sup> ions are introduced, the PL property have been further enhanced, and the PL intensity can up to 1.8 times as high of that BAM specimen obtained by the HTS method. The xy CIE chromaticity coordinates of SBAM: 0.1Eu<sup>2+</sup>, 0.04Mn<sup>2+</sup> phosphor is presented at (0.146, 0.250), located at the blue-green reign.

**Keywords:** solution combustion synthesis; BAM:Eu<sup>2+</sup>, Mn<sup>2+</sup>; optical material; blue-green phosphor

收稿日期: 2016-04-01。收修改稿日期: 2016-09-20。

国家自然科学基金(No.51472162)、上海应用技术大学引进人才启动基金(No.YJ2015-32)和 2016 年度上海市“联盟计划”项目(No.LM201623)资助

\*通信联系人。E-mail: nzhang@sit.edu.cn, jianyong1106@163.com, Tel: +86 13564362742, 13761207951

Conventionally,  $\text{BaMgAl}_{10}\text{O}_{17}$  (BAM) phosphor is obtained via an energy greedy solid-state reaction route<sup>[1]</sup>, at high temperature (above 1 300 °C) for several hours. Whereas, the solid-state method has some shortcomings such as the process complexity, energy-consuming, inhomogeneous mixing and contamination by impurities, and the product resulting in big size range and irregular shapes, inappropriate for the devices foreseen<sup>[2-3]</sup>. Thereby, this synthesis route seems to be an encouraging method to prepare efficient small-sized phosphors. Many wet-chemical methods have been carried out to prepare phosphors, such as co-precipitation<sup>[4]</sup>, sol-gel<sup>[5]</sup> and combustion synthesis<sup>[6-7]</sup>. Therein, there are several advantages of the combustion synthesis technique. Firstly, this combustion synthesis technique makes use of the heat energy liberated by the redox exothermic reaction at a relative low temperature, which is the igniting temperature between metal nitrates and urea or other fuels. Secondly, the high temperature generated instantly by exothermic reaction can volatilize low boiling point impurities. Thirdly, it is conducted in liquid phases, so that each component can be accurately controlled and uniformly mixed. In one word, combustions synthesis can produce high pure and well-crystallized oxides at significantly lower temperatures within a short duration. Thus, ultrafine  $\text{BAM:Eu}^{2+}$  has been prepared in the literatures by the corresponding metal nitrate-urea mixture synthesis<sup>[8-12]</sup>. However, the emission of  $\text{Mn}^{2+}$  is strongly affected by the crystal field of the host materials<sup>[13-14]</sup>. At the same time, the  $\text{Mn}^{2+}$  is susceptible to oxygen and could cause the specimen turn gray or black, this could dramatically cause decrease of the photoluminescence. Thus, the combustion preparation of  $\text{BAM:Eu}^{2+}$ ,  $\text{Mn}^{2+}$  phosphor has not been reported. In addition, Sr, Ba and Mg elements are comparable, except for the difference of diameter. Thus, the introduction of  $\text{Sr}^{2+}$  ions is expected to improve the optical property of BAM<sup>[15]</sup>.

In this paper, urea and polyethylene glycol 600 (PEG 600) are chosen as fuel or template to prepare the  $\text{BaMgAl}_{10}\text{O}_{17}$  (BAM):  $\text{Eu}^{2+}$ ,  $\text{Mn}^{2+}$ ,  $\text{Sr}^{2+}$  phosphor by solution combustion synthesis (SCS). The structural, morphological and optical properties of  $\text{BAM:Eu}^{2+}$ ,

$\text{Mn}^{2+}$ ,  $\text{Sr}^{2+}$  powders are studied by means of X-ray diffraction (XRD), scanning electron microscopy (SEM) and photoluminescence (PL) spectra.

## 1 Experimental

### 1.1 Materials and physical measurements

All the starting materials were of analytical grade as obtained from commercial sources and used without further purification. The structures of the samples were characterized on X-ray diffraction (Shimadzu, XD-3A) at 35 kV, 25mA for a  $\text{Cu K}\alpha$  radiation ( $\lambda = 0.154\ 18\ \text{nm}$ ) over the  $2\theta$  range of  $10^\circ \sim 80^\circ$  at room temperature. The morphology of the samples were obtained on field emission scanning electron microscope (SEM, Hitachi, S-4800). The excitation and emission spectra were recorded on an F-7000 fluorescence spectrophotometer.

### 1.2 Syntheses of different powders

$\text{Sr}_{0.05}\text{Ba}_{0.85}\text{Mg}_{0.96}\text{Al}_{10}\text{O}_{17}$  (SBAM):  $0.1\text{Eu}^{2+}$ ,  $0.04\text{Mn}^{2+}$  powder was prepared by SCS method with CO ( $\text{NH}_2$ )<sub>2</sub> as fuel and  $\text{Sr}(\text{NO}_3)_2$ ,  $\text{Ba}(\text{NO}_3)_2$ ,  $\text{Mg}(\text{NO}_3)_2 \cdot 6\text{H}_2\text{O}$ ,  $\text{Al}(\text{NO}_3)_3 \cdot 9\text{H}_2\text{O}$ ,  $\text{Mn}(\text{NO}_3)_2$  and  $\text{Eu}(\text{NO}_3)_3 \cdot 5\text{H}_2\text{O}$  as metallic precursors. Metal nitrates were weighed stoichiometrically, dissolved in distilled water in a corundum crucible and stirred in order to obtain a clear solution. It was pointed that the stoichiometric molar ratio of urea to nitrates was 6:1 in this case and the concentration of PEG-600 was 5%, which played an important role in the combustion reaction to obtain the reductive environments. After full stirring, the precursor solution was introduced into a muffle furnace maintained at 600 °C. Initially, the solution boiled, underwent dehydration followed by decomposition with the evolution of large amounts of gases and burst into flames, then, spontaneous combustion with enormous swelling, producing white foamy and voluminous phosphor. The whole process spent 5 minutes and resulted into a foamy white powder.

## 2 Results and discussion

### 2.1 XRD patterns and the simulated structure of SBAM

XRD patterns of the different BAM based

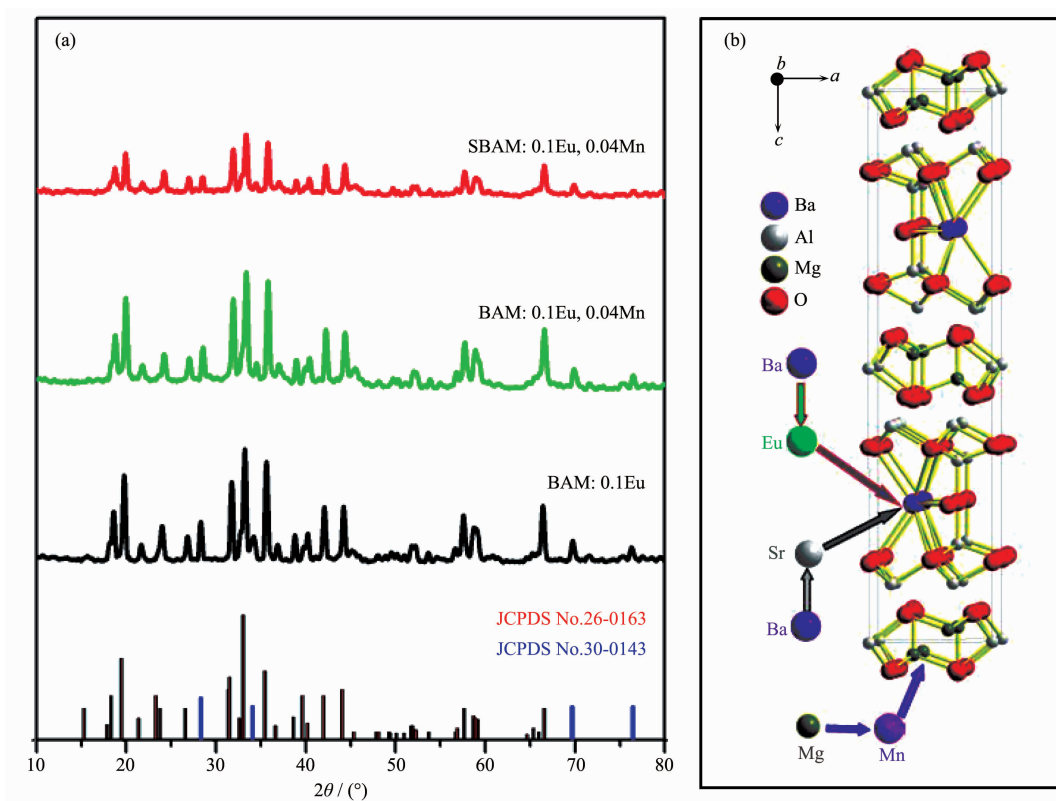


Fig.1 XRD patterns of different powders (a) and the simulated crystal structure of the SBAM sample (b)

phosphors are presented in Fig.1(a). Almost the curves are in excellent agreement with the pattern of barium magnesium aluminate (BAM). The ideal peak positions and intensities for hexagonal BAM (JCPDS No.26-0163 are marked at the bottom), are corresponding to the space group  $P6_3/mmc$  (No.194). The obtained phosphors are monophasic BAM except for the impurity with BaO (JCPDS No.30-0143), which would not influence the optical property of the samples. Furthermore, these samples show the iso-structure with the solid-reacted sample<sup>[16]</sup>, but the broadening patterns are observed in nanoparticles. The data distinguishes that the SBAM: 0.1Eu<sup>2+</sup>, 0.04Mn<sup>2+</sup> phosphor has been successfully synthesized with the fast SCS method.

As shown in Fig.1(b), the simulated structure of SBAM: 0.1Eu<sup>2+</sup>, 0.04Mn<sup>2+</sup>, the Eu<sup>2+</sup> ions partially replace Ba ions, occupying the 2d site (1/3, 2/3, 3/4), and Ba<sup>2+</sup> ions have taken place by the Sr<sup>2+</sup> in the mirror plane. Meanwhile, the activator Mn<sup>2+</sup> ions substituted Mg<sup>2+</sup> ions is incorporated into the spinal blocks instead into the conduction layers. Herein, a

strong crystal field is generated when Eu<sup>2+</sup> ions is located at a site with a distorted co-ordination field. The interatomic distance between cation and adjacent oxygen atoms are changed and the PL property could consequently vary.

## 2.2 Morphological analysis of SBAM: 0.1Eu<sup>2+</sup>, 0.04Mn<sup>2+</sup>

The microstructures of SBAM: 0.1Eu<sup>2+</sup>, 0.04Mn<sup>2+</sup> phosphor are studied on their SEM and TEM micrographs (Fig.2). As shown in Fig.2 (a), the surfaces of the foams show a lot of cracks voids and pores, which can be correlated with the exothermic character of the combustion reaction. The most of rod-like SBAM: 0.1Eu<sup>2+</sup>, 0.04Mn<sup>2+</sup> are unambiguously identified on SEM image (Fig.2b). In order to achieve accurate data of the grain size of SBAM: 0.1Eu<sup>2+</sup>, 0.04Mn<sup>2+</sup> powder, its TEM image is recorded in Fig.2c. Typically, the diameter of individual rods is *ca.* 20 nm, whereas their length is about 200 ~500 nm. Besides, the few particles seem to have the average diameter of *ca.* 25 nm. It can be deduced that the SCS process has advantages on avoiding the agglomeration of nanorods

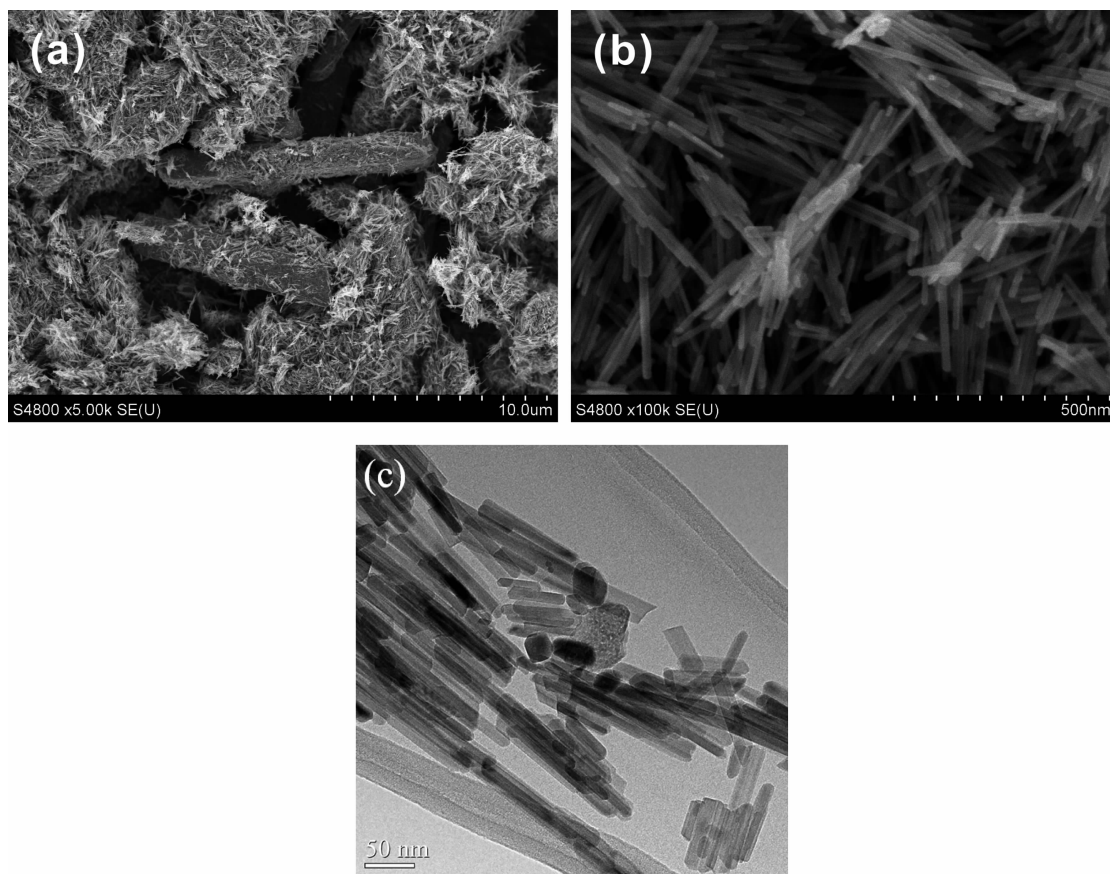


Fig.2 SEM images (a, b) and TEM image (c) of SBAM: 0.1Eu<sup>2+</sup>, 0.04Mn<sup>2+</sup>

and nanoparticles, and the addition of PEG can increase the viscosity of solution to obtain rod-like feature.

### 2.3 PL properties

From Fig.3(a) and (b), it shows that the emission band of Eu<sup>2+</sup> ions overlaps the excitation peaks of Mn<sup>2+</sup> ions, suggesting that the emitted photons of Eu<sup>2+</sup> ions can be reabsorbed by Mn<sup>2+</sup> ions, and the energy transfer from Eu<sup>2+</sup> to Mn<sup>2+</sup> can be occurred. In order to investigate the influence of Mn<sup>2+</sup> on the blue and green BAM phosphor, a series of the emission spectra for BAM: 0.1Eu<sup>2+</sup>, *x*Mn<sup>2+</sup> (*x*=0.01, 0.04, 0.08, 0.10 and 0.12) samples are prepared by the SCS route. As shown in Fig.3(c), at the initial Mn concentration (1%), the PL intensity at 450 nm of prepared samples are comparable with the commercial blue phosphors (0%, Mn<sup>2+</sup>). Meanwhile, it is found that all the samples have a very strong emission band peaking at 450 nm with a full-width half-maximum (FWHM) of 52 nm, which is translated to that Eu<sup>2+</sup> ions have incorporated

at barium sites within the intermediate layers, and the 4*f*<sup>6</sup>5*d*<sup>1</sup>-4*f*<sup>7</sup> transition of the Eu<sup>2+</sup> ions results in the strong blue emission<sup>[17-18]</sup>. Meanwhile, the 335 nm excitation produces a green emission band located at 514 nm, attributed to the <sup>4</sup>T<sub>1</sub>-<sup>6</sup>A<sub>1</sub> transition of Mn<sup>2+</sup> with the FWHM of 25 nm, which means that the Mn<sup>2+</sup> substitutes Mg<sup>2+</sup> and incorporates into the spinel blocks, instead into the conduction layers<sup>[19-20]</sup>. In Fig.3(d), the emission intensity of the 514 nm increases with increasing Mn<sup>2+</sup> concentration, followed by the decrease of Eu<sup>2+</sup> emission intensities, which reflects that the energy transfer from Eu<sup>2+</sup> to Mn<sup>2+</sup> have taken place. The intensity of green emission peak (514 nm) reaches a maximum when the ratio of Mn<sup>2+</sup> is 8% (molar ratio). When *x* value is higher than 0.08, the specimen become gray, which can be explained that the Mn<sup>2+</sup> is susceptible to oxygen, and the reduction extent during the SCS is not sufficient. The deep color influences the luminescence property. Thus, the luminescence intensity shows dramatic decrease. The above results

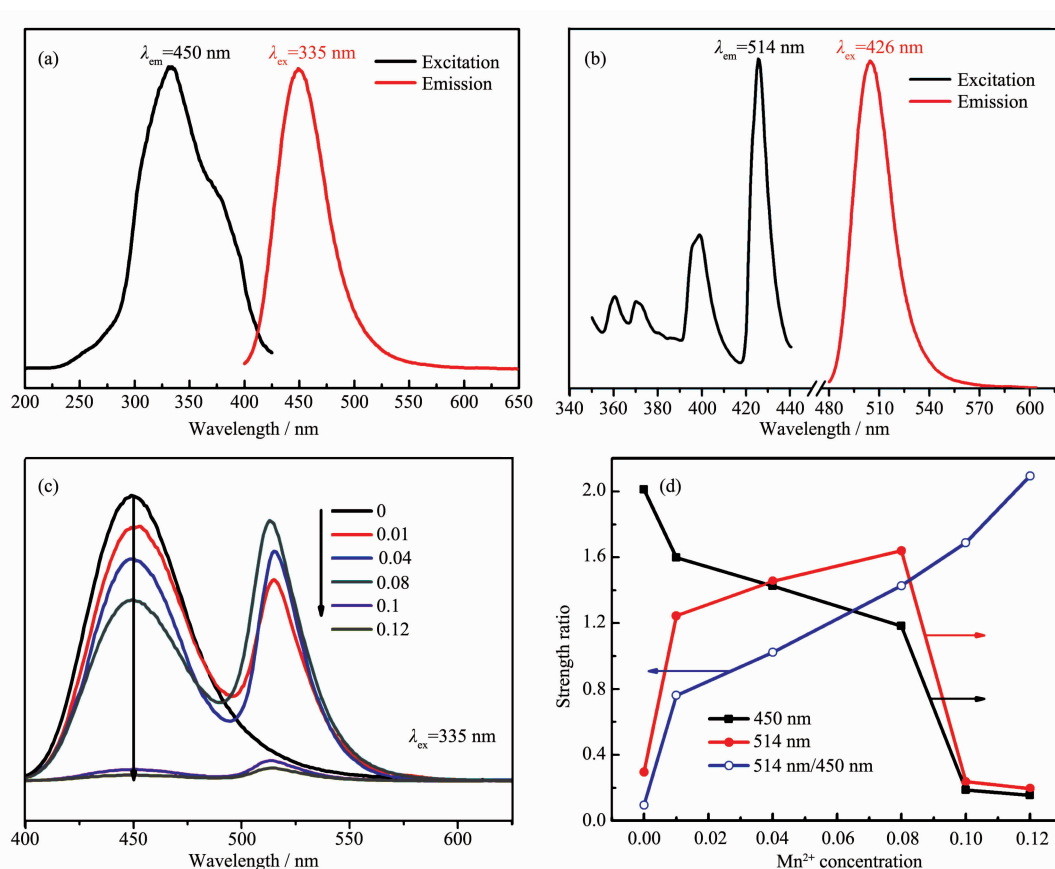


Fig.3 Excitation and emission spectra of (a) BAM: 0.1Eu<sup>2+</sup> (b) BAM: 0.04Mn<sup>2+</sup> (c) Emission spectra of BAM: 0.1Eu<sup>2+</sup>, xMn<sup>2+</sup>, (d) relative emission intensity and the ratio of 514 nm/450 nm as a function of Mn<sup>2+</sup> concentration

confirm that the concentration quench appears, due to the shorter distance of the light center. In addition, with increasing the concentration of Mn<sup>2+</sup>, the intensity ratio of the green band of Mn<sup>2+</sup> to the blue band of Eu<sup>2+</sup> becomes larger. It reveals that the energy diffusion between donors, which speeds up the average transfer rate to Mn<sup>2+</sup> acceptors.

Furthermore, to improve the PL property of the BAM: 0.1Eu<sup>2+</sup>, 0.04Mn<sup>2+</sup>. The small Sr<sup>2+</sup> ions ( $r=0.120 \text{ nm}$ ) are expected to be inserted into the crystal lattice to substitute the larger Ba<sup>2+</sup> ions ( $r=0.138 \text{ nm}$ ), and the crystal cell diameter would decrease as shown in Fig.1. As a result, the extend of closed-pack of Eu<sup>2+</sup> as a luminescence center and the surrounding O<sup>2-</sup> increase, which means that the Sr substitution into Ba sites reduces not only the excitation near the band edge at wavelengths but also the charge transfer of excitation to the conduction layer. Consequently, the PL intensity of SBAM: 0.1Eu<sup>2+</sup>, 0.04Mn<sup>2+</sup> phosphor is

improved in comparison with BAM sample, which is corresponding to the previous report<sup>[21]</sup>. One fact is that there is no change in the peak position of the emission spectra, which suggests that the crystal field of the host matrix are not affected by the change of the conduction layers from BaO to SrO. With increasing Sr<sup>2+</sup> concentration, the PL intensity increases and reaches a maximum at 5%, which is about 1.4 times as high as that of the BAM: 0.04Mn<sup>2+</sup>, 0.1Eu<sup>2+</sup> specimen (shown in Fig.4a). The result can be translated to the synergy effect by substituting Sr for Ba in the conduction layers.

As shown in Fig.4(b), with the increase of the Sr<sup>2+</sup> concentration, the intensity ratio of the blue band of Eu<sup>2+</sup> to the green band of Mn<sup>2+</sup> declines. It can be deduced that the Sr<sup>2+</sup> substitution improves the excitation efficiency of the spinel blocks, simultaneously reducing the efficiency for the charge-transfer transition and the excitation in the conduction layer.



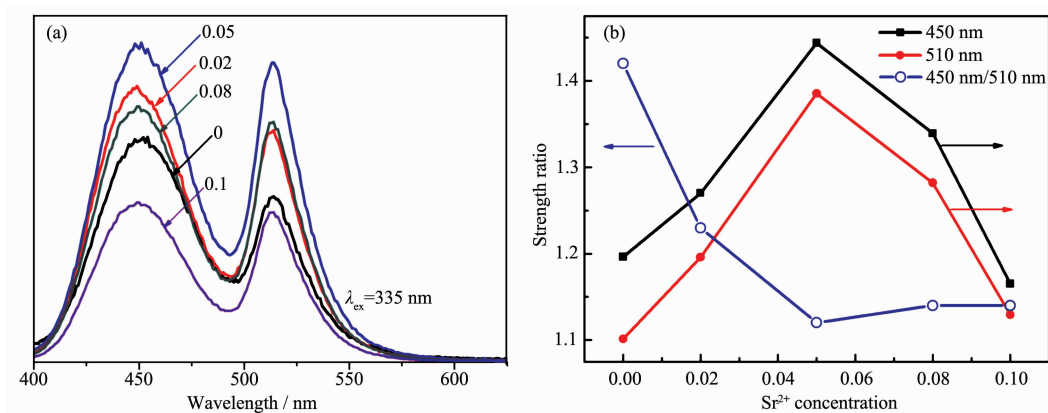


Fig.4 (a) Emission spectra of BAM:  $\gamma\text{Sr}^{2+}$ ,  $0.1\text{Eu}^{2+}$ ,  $0.04\text{Mn}^{2+}$  and (b) the relative emission intensity at 450 nm / 514 nm as a function of  $\text{Sr}^{2+}$  concentration

It also means that  $\text{Sr}^{2+}$  ions make the energy transfer from  $\text{Eu}^{2+}$  to  $\text{Mn}^{2+}$  easy, and the luminescent intensity of  $\text{Mn}^{2+}$  is improved to a large degree. Lower doping concentrations and excessive doping of  $\text{Sr}^{2+}$  lead to the luminescent intensity decreases and concentration quenching of the blue or green emission, respectively. In this case, it is proposed that the concentration quenching is caused by an energy transfer process between  $\text{Eu}^{2+}$ - $\text{Eu}^{2+}$  or  $\text{Mn}^{2+}$ - $\text{Mn}^{2+}$  ions. In accordance with this point of view, the desirable doping level of  $\text{Sr}^{2+}$  is 5%.

Fig.5(a) shows the emission spectra of as-prepared samples with different methods. It is found that the PL property of BAM:  $0.1\text{Eu}^{2+}$ ,  $0.04\text{Mn}^{2+}$  material shaped by SCS method is superior to that by the HTS reaction. The well-dispersed morphology of the SCS-

derived phosphors is beneficial to the improvement of PL property. While  $\text{Sr}^{2+}$  ions are introduced, the PL property have been further enhanced due to the distorted co-ordination field and PL intensity can up to 1.8 times as high of that BAM specimen obtained by the HTS method. To explore the material performance on color luminescent emission,  $xy$  CIE chromaticity coordinates are obtained from calculation based on the emission spectra, shown in Fig.5(b). For BAM (HTS), BAM (SCS) and SBAM (SCS), the data were S0 (0.151, 0.181), S1 (0.146, 0.201) and S2 (0.146, 0.250), respectively, which relate to green-blue color. Therefore, for SBAM:  $0.1\text{Eu}^{2+}$ ,  $0.04\text{Mn}^{2+}$ , phosphor, when combining red phosphors, a white emission is expected to be obtained.

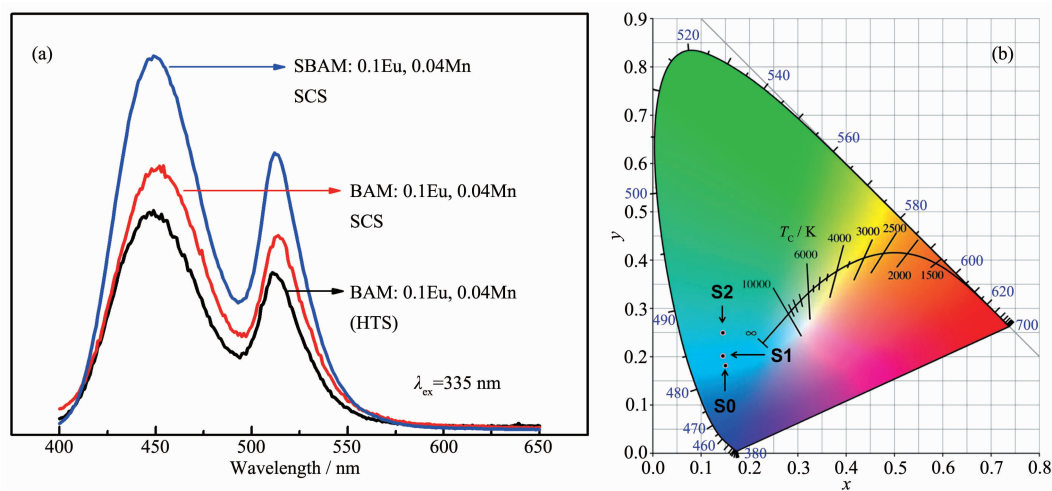


Fig.5 Emission spectra of different powder (a) and (b) the corresponding CIE chromaticity diagram of S0 (BAM:  $0.1\text{Eu}^{2+}$ ,  $0.04\text{Mn}^{2+}$  (HTS)), S1 (BAM:  $0.1\text{Eu}^{2+}$ ,  $0.04\text{Mn}^{2+}$  (SCS)) and S2 (SBAM:  $0.1\text{Eu}^{2+}$ ,  $0.1\text{Mn}^{2+}$  (SCS))

### 3 Conclusions

SBAM: Eu<sup>2+</sup>, Mn<sup>2+</sup> phosphors are successfully fabricated using SCS method at 600 °C for 5 min. Analytical results show that the SBAM: 0.1Eu<sup>2+</sup>, 0.04Mn<sup>2+</sup> phosphors have well crystallized BAM phase, with the most nanorods diameter of 20 nm, length of 200~500 nm, and fewer nanoparticles size of 25 nm. From the PL measurement, it is clearly seen that the co-doping (Eu<sup>2+</sup>, and Sr<sup>2+</sup> ions) in the BAM: Mn<sup>2+</sup> host have significantly improved the emission intensity, as a consequence of the energy transfer from Eu<sup>2+</sup> ion in the conduction layers to Mn<sup>2+</sup> in the spinal blocks, and the distorted co-ordination field. From the CIE chromaticity coordinates data, it is found that SBAM: 0.1Eu<sup>2+</sup>, 0.04Mn<sup>2+</sup> powder locates at the center of blue-green region. All these results indicate that SBAM: Eu<sup>2+</sup>, Mn<sup>2+</sup> prepared by the SCS method as a promising blue-green phosphor can be widely applied in white light LEDs.

**Acknowledgements:** This work is supported by the Key discipline grant for composite materials from Shanghai Institute of Technology (Grant No.10210Q140001), the starting up foundation from Shanghai Institute of Technology (Grant No. YJ2015-32) and the National Natural Science Foundation of China (Grant No.51472162, 21503081).

### References:

- [1] WU Jiang(吴疆), ZHANG Ping(张萍), JIANG Chun-Dong(蒋春东), et al. *Chinese J. Inorg. Chem.*(无机化学学报), **2015**, **31**(6):1201-1206
- [2] Zhang Z H, Wang Y H, Li X X, et al. *J. Lumin.*, **2007**,**122**: 1003-1005
- [3] Wu Z, Dong Y, Jiang J. *J. Alloys Compd.*, **2009**,**467**(1):605-610
- [4] Zhang Z H, Feng J G, Huang Z L. *Particuology.*, **2010**,**8**(5): 473-476
- [5] Lu C H, Chen C T. *J. Rare Earth.*, **2006**,**24**(6):706-711
- [6] Pradal N, Potdevin A, Chadeyron G, et al. *Mater. Res. Bull.*, **2011**,**46**(4):563-568
- [7] Luo Z L, Geng B, Bao J, et al. *J. Comb. Chem.*, **2005**,**7**:942-946
- [8] Chen Z, Yan Y. *J. Mater. Sci.*, **2006**,**41**(17):5793-5796
- [9] Chen Z, Yan Y W, Liu J M, et al. *J. Alloys Compd.*, **2009**, **478**:679-683
- [10] DENG Sheng-Zhi(邓升智), LIU Chen(刘晨), YANG Chu-Jun(杨楚珺), et al. *Chinese J. Inorg. Chem.*(无机化学学报), **2015**,**31**(2):229-236
- [11] LÜ Xing-Dong(吕兴栋), SHU Wan-Gen(舒万艮). *Chinese J. Inorg. Chem.*(无机化学学报), **2006**,**22**(5):808-812
- [12] WANG Fei(王飞), TIAN Yi-Guang(田一光), ZHANG Qiao(张乔). *Chinese J. Inorg. Chem.*(无机化学学报), **2014**,**30** (11):2530-2536
- [13] Kim Y, Kang S. *Appl. Phys. B*, **2010**,**98**(2/3):429-434
- [14] You H, Zhang J, Hong G, et al. *J. Phys. Chem. C*, **2007**,**111** (28):10657-10661
- [15] XIE Yong-Rong(谢永荣), ZHONG Hai-Shan(钟海山), YUAN Xiao-Yong(袁小勇), et al. *Chinese J. Inorg. Chem.*(无机化学学报), **2006**,**22**(8):1550-1554
- [16] Yang P, Yao G Q, Lin J H. *Opt. Mater.*, **2004**,**26**(3):327-331
- [17] Setlur A A, Shiang J J, Happek U. *Appl. Phys. Lett.*, **2008**, **92**(8):081104
- [18] Zhang J, Zhou M, Liu B, et al. *Int. J. Appl. Ceram. Technol.*, **2013**,**10**(4):638-642
- [19] Zhang J, Zhou M, Liu B Y, et al. *J. Lumin.*, **2012**,**132**(8): 1949-1952
- [20] Kim K B, Kim Y I, Chun H G, et al. *Chem. Mater.*, **2002**,**14** (12):5045-5052
- [21] Jung K Y, Lee H W, Kang Y C, et al. *Chem. Mater.*, **2005**, **17**:2729-2734